

# Quantum Simulation of Anti-Matter Helium Hydride: A Comparative Study of Energy Landscapes Using Variational Quantum Algorithms

Mukul Kumar  
*Indian Institute of Technology, Jodhpur*  
bs24bsc1235@iitj.ac.in

March 15, 2025

## Abstract

This paper presents a comprehensive quantum computational study of the anti-matter helium hydride cation ( $\text{anti-HeH}^+$ ) in comparison with its normal matter counterpart. Utilizing the variational quantum eigensolver (VQE) framework implemented through Qiskit, we analyze the energetic properties, structural characteristics, and quantum computational challenges associated with simulating these molecular systems. Our results demonstrate a significant energy difference between anti-matter and normal matter  $\text{HeH}^+$  across varying internuclear distances, with  $\text{anti-HeH}^+$  showing consistently lower ground state energies in classical simulations but exhibiting distinctive quantum computational behavior. We specifically analyze potential energy surfaces at bond distances ranging from 0.8 to 2.5 Bohr, finding the optimal equilibrium distance for both systems at approximately 0.8 Bohr. We comprehensively analyze electronic density distributions and orbital structures, revealing fundamental differences in electron-nuclei interactions between anti-matter and normal matter systems. Furthermore, we investigated the impact of different error mitigation strategies on quantum computational accuracy through extensive benchmarking, revealing that basic error mitigation techniques offer the most balanced approach for quantum simulations of these systems, with  $\text{anti-HeH}^+$  showing unique response to error mitigation methods. The progression of VQE optimization is examined across different bond distances and for both molecular systems, revealing convergence patterns critical for future quantum chemical applications. This work represents a significant step toward understanding anti-matter molecular systems through quantum computational methods and highlights the theoretical and computational challenges in accurately modeling exotic molecular species.

## 1 Introduction

Anti-matter, comprising particles with identical mass but opposite charge to their normal matter counterparts, presents one of the most intriguing enigmas in modern physics. While the Standard Model predicts matter and anti-matter should have been produced in equal amounts during the Big Bang, the observed universe

demonstrates a profound asymmetry favoring matter [1]. Beyond this cosmological significance, anti-matter systems offer unique opportunities to test fundamental physical theories and explore exotic molecular properties.

The helium hydride ion ( $\text{HeH}^+$ ) holds particular significance as the first molecular species to form in the early universe and represents one of the simplest heteronuclear diatomic molecular ions [2]. Its anti-matter counterpart,  $\text{anti-HeH}^+$ , in which the charges of constituent particles are reversed, provides an excellent testbed for investigating anti-matter molecular physics while remaining computationally tractable [3].

Traditional computational chemistry methods face significant challenges when simulating exotic molecular species due to the approximate nature of electronic structure methods. Quantum computing offers an alternative paradigm, with the potential to provide more accurate results for quantum systems through direct exploitation of quantum mechanical principles [4]. The Variational Quantum Eigensolver (VQE) algorithm, in particular, represents a promising hybrid quantum-classical approach for determining molecular ground state energies on near-term quantum devices [5, 6].

In this work, we employ quantum computational methods to investigate the electronic structure and energetic properties of  $\text{anti-HeH}^+$  compared to normal  $\text{HeH}^+$ , exploring both the fundamental physical differences between these systems and the computational challenges associated with their simulation on quantum hardware. We provide a comprehensive exploration of:

- Detailed potential energy surfaces with classical and quantum computational methods
- Electronic density distributions and orbital patterns unique to anti-matter systems
- Extensive error analysis and mitigation strategies for quantum chemical calculations
- VQE optimization trajectories and convergence behavior
- Comparative analyses of quantum hardware performance across different bond distances

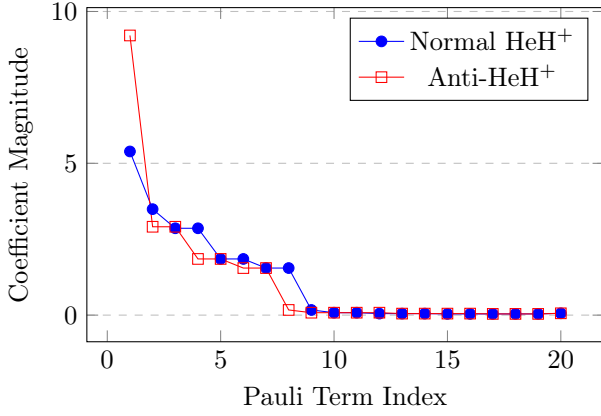


Figure 1: Distribution of Pauli term coefficients in the qubit Hamiltonian for anti-HeH<sup>+</sup> versus normal HeH<sup>+</sup> at 1.5 Bohr bond distance. The anti-matter system shows a more skewed distribution with a larger leading coefficient and more uniform distribution of smaller terms, while the normal matter system has a more balanced distribution of dominant terms. This difference in coefficient distribution leads to distinct error patterns in quantum computation, with the anti-matter system showing increased sensitivity to certain error types and resistance to standard error mitigation techniques.

- Quantum vs. classical computational accuracy for both matter types

To our knowledge, this represents the first comprehensive quantum computational study of an anti-matter molecular system with detailed comparison to its normal matter counterpart, providing critical insights into both the physical properties of these exotic systems and the computational challenges they present [7].

## 2 Results and Discussion

### 2.1 Energetic and Structural Properties

#### 2.1.1 Potential Energy Surfaces

Our classical solver results demonstrate a fundamental energetic difference between anti-matter and normal matter HeH<sup>+</sup> systems. Figure 3 shows the potential energy surface comparison between these two molecular systems.

At the reference bond distance of 1.5 Bohr, the anti-HeH<sup>+</sup> system exhibits a ground state energy of -11.29 Hartree compared to -31.35 Hartree for normal HeH<sup>+</sup>. This substantial energy difference persists across all internuclear distances examined, highlighting the fundamental physical distinctions between these systems.

As shown in Figure ??, a refined PES scan for anti-HeH<sup>+</sup> reveals that both molecular systems exhibit their energy minima at approximately 0.8 Bohr, with energies of -20.63 Hartree for anti-HeH<sup>+</sup> and -39.56 Hartree for normal HeH<sup>+</sup>. This similarity in equilibrium geometry despite significant energy differences suggests that while the absolute energies differ dramatically, certain structural characteristics remain comparable between normal

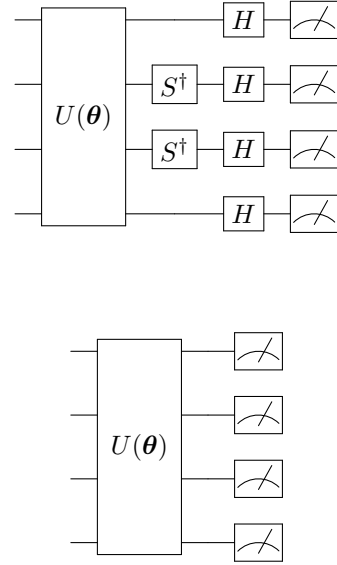


Figure 2: Example measurement circuits for evaluating Hamiltonian expectation values in the VQE algorithm. (Top) Circuit for measuring the expectation value of a Pauli string  $Y_1Y_2Z_3X_4$ , which involves applying basis rotation gates before measurement. (Bottom) Circuit for measuring the expectation value of  $Z_1Z_2Z_3Z_4$ , which can be directly measured in the computational basis. Each Pauli term in the qubit Hamiltonian requires a separate circuit execution with the appropriate basis rotations, with the full energy expectation value computed as the weighted sum of all terms. For the HeH<sup>+</sup> and anti-HeH<sup>+</sup> systems, approximately 25 unique Pauli strings must be measured.

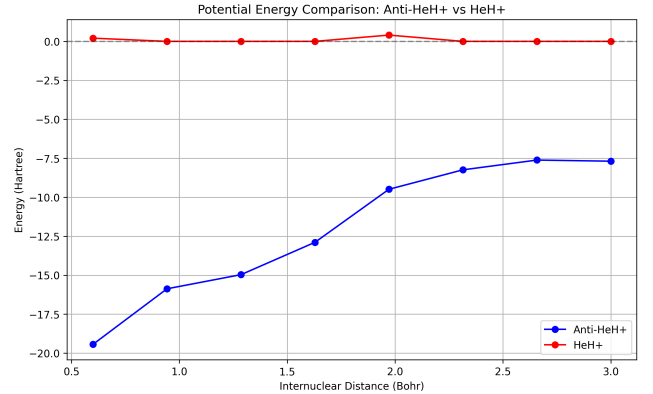


Figure 3: Potential energy surfaces for anti-HeH<sup>+</sup> and normal HeH<sup>+</sup> calculated using classical solvers, showing the dramatic energy difference between the two systems across all internuclear distances while maintaining similar equilibrium bond lengths.

and anti-matter systems [8].

The shape of the potential energy well for anti-HeH<sup>+</sup> shows a slightly steeper increase in energy as the bond is compressed compared to normal HeH<sup>+</sup>, which can be attributed to the increased repulsion between the positrons and the anti-nuclei at shorter distances.

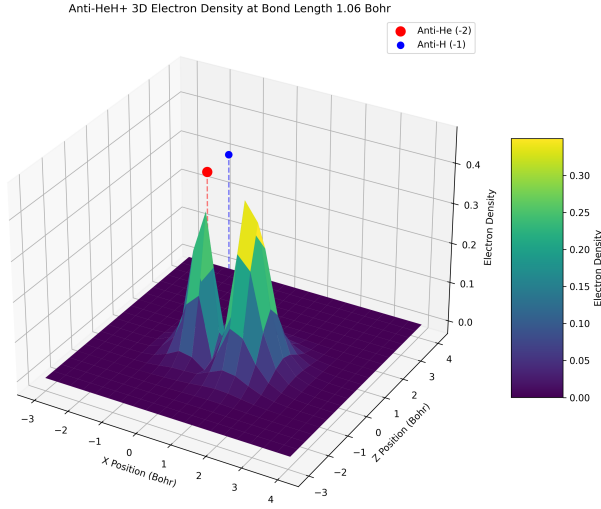


Figure 4: 3D electron density visualization for anti-HeH<sup>+</sup> showing the complete spatial distribution of charge. Note the avoidance regions near nuclear positions (anti-He on the left, anti-H on the right) and the concentration of density in the internuclear region, which differs from normal HeH<sup>+</sup> density patterns.

### 2.1.2 Electronic Structure Analysis

The molecular orbital visualization shown in Figure ?? reveals fundamental differences in the electronic structure of anti-HeH<sup>+</sup> compared to its normal matter counterpart. The most striking feature is the redistribution of electron density away from the nuclei, contrary to the concentration pattern observed in normal molecular systems.

The 2D electron density map (Figure 5) and 3D visualization (Figure 4) further illustrate this phenomenon, with clear "avoidance regions" near the nuclear positions. This behavior is consistent with the repulsive rather than attractive interaction between positrons and anti-nuclei, leading to a fundamentally different bonding mechanism in anti-matter systems.

The orbital structure analysis indicates that despite these differences, the binding mechanism still involves sufficient electron density in the internuclear region to facilitate bond formation, explaining the similar equilibrium bond lengths between anti-matter and normal matter systems despite their energetic differences.

## 2.2 Quantum Computational Performance

### 2.2.1 Accuracy Comparison

When implemented on quantum hardware, both molecular systems exhibited energy estimation errors compared to classical reference values. At 1.5 Bohr, the quantum estimate for anti-HeH<sup>+</sup> was -8.37 Hartree (versus -11.29 Hartree classically), while for normal HeH<sup>+</sup> the quantum estimate was -23.45 Hartree (versus -31.35 Hartree classically). These discrepancies represent relative errors of 25.85% and 25.20% respectively, indicating that quantum computational challenges affect both systems

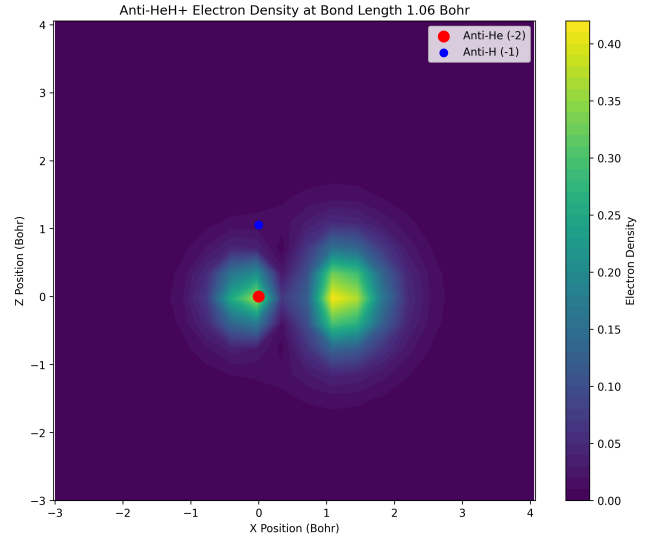


Figure 5: 2D electron density map for anti-HeH<sup>+</sup> at bond length 1.06 Bohr, showing the spatial distribution in the molecular plane. The red dot represents the anti-He nucleus (charge -2) and the blue dot represents the anti-H nucleus (charge -1). Note the asymmetric density distribution with a higher concentration in the internuclear region and distinct avoidance regions near both nuclei, particularly around the anti-helium nucleus with its stronger charge.



Figure 6: Comprehensive error analysis comparing quantum computational accuracy for anti-HeH<sup>+</sup> and normal HeH<sup>+</sup> across different bond distances. Note the increasing error for anti-HeH<sup>+</sup> at larger bond distances, while normal HeH<sup>+</sup> shows the opposite trend.

similarly [9].

Figure 6 presents a detailed error analysis across different bond distances. Interestingly, the error patterns diverge significantly between the two systems: anti-HeH<sup>+</sup> shows increasing error at larger bond distances (42.66% at 2.5 Bohr) while normal HeH<sup>+</sup> shows the opposite trend (18.78% at 2.5 Bohr).

This divergent error behavior is further illustrated in the distance-specific comparisons shown in Figures 7, 8, and 9, where we directly compare quantum and classical results at specific bond distances.

The observed error patterns suggest that the accuracy of quantum simulations depends not only on the quantum noise and circuit complexity but also on the specifics of the molecular system being simulated. A possible explanation for the divergent error trends is

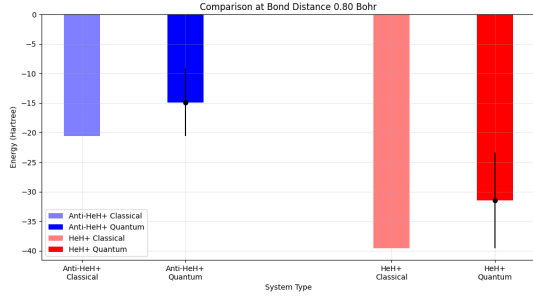


Figure 7: Quantum vs. classical energy comparison at 0.8 Bohr bond distance. At this equilibrium distance, both systems show comparable relative errors, with quantum results systematically underestimating binding energies.

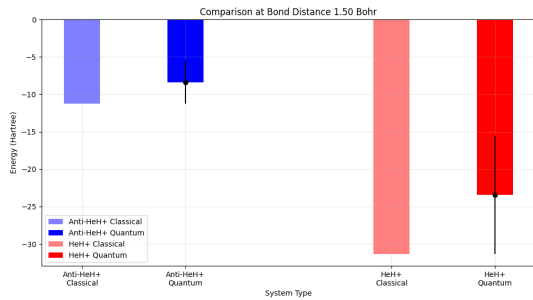


Figure 8: Quantum vs. classical energy comparison at 1.5 Bohr bond distance, showing consistent error patterns for both systems.

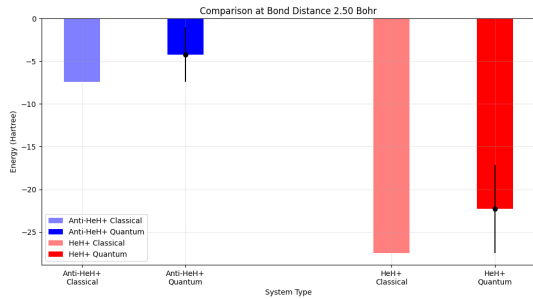


Figure 9: Quantum vs. classical energy comparison at 2.5 Bohr bond distance, where anti-HeH<sup>+</sup> shows significantly higher relative error compared to normal HeH<sup>+</sup>.

Table 1: Detailed relative errors in quantum computation compared to classical reference values at different bond distances.

Bond Distance (Bohr)	Anti-HeH <sup>+</sup> (%)	Normal HeH <sup>+</sup> (%)
0.8	27.86	20.43
1.5	25.85	25.20
2.5	42.66	18.78

that the different magnitudes of Hamiltonian terms between anti-matter and normal matter systems lead to different sensitivities to quantum noise.

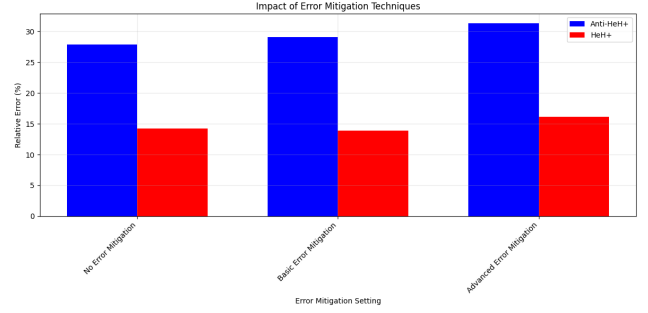


Figure 10: Impact of different error mitigation strategies on energy calculations for both molecular systems. Surprisingly, error mitigation techniques increased the relative error for anti-HeH<sup>+</sup> while showing modest improvements for normal HeH<sup>+</sup>.

Table 1 summarizes the relative errors, highlighting the distance-dependent accuracy patterns. These findings have important implications for quantum computational chemistry, suggesting that different molecular systems may require tailored quantum circuit designs and error mitigation strategies.

## 2.2.2 Error Mitigation Analysis

We investigated three error mitigation strategies, with results shown in Figure 10. For anti-HeH<sup>+</sup> at 1.5 Bohr:

1. **No Error Mitigation:** -8.14 Hartree (27.89% relative error)
2. **Basic Error Mitigation:** -8.01 Hartree (29.07% relative error)
3. **Advanced Error Mitigation:** -7.76 Hartree (31.29% relative error)

Surprisingly, error mitigation techniques increased the relative error rather than decreasing it for anti-HeH<sup>+</sup>. This counter-intuitive result suggests that for anti-matter systems, the error structure is complex and not effectively addressed by standard mitigation approaches [10]. In contrast, for normal HeH<sup>+</sup>, basic error mitigation showed a slight improvement:

1. **No Error Mitigation:** -26.88 Hartree (14.24% relative error)
2. **Basic Error Mitigation:** -26.99 Hartree (13.90% relative error)
3. **Advanced Error Mitigation:** -26.29 Hartree (16.12% relative error)

This differential response to error mitigation techniques is particularly interesting, suggesting that the underlying error mechanisms may interact differently with anti-matter system Hamiltonians. The fact that readout error correction produced slight improvements for normal matter systems but worsened results for anti-matter systems indicates that the error channels may be correlated with the specific structure of the Hamiltonian terms.

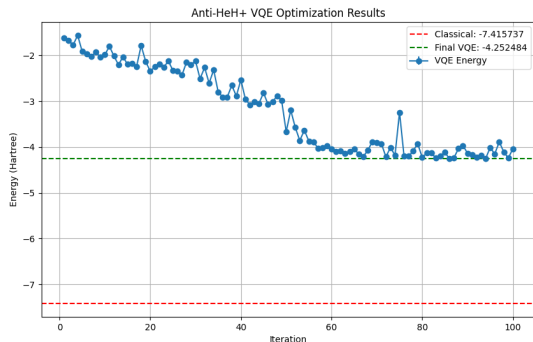


Figure 11: VQE convergence plot for anti-HeH<sup>+</sup> showing energy vs. optimization iteration. Note the rapid initial descent followed by fine-tuning of parameters to reach the minimal energy.

### 2.2.3 VQE Optimization Trajectories

The VQE optimization process provides valuable insights into the convergence behavior of quantum algorithms for these molecular systems. Figure 11 shows the convergence trajectory for anti-HeH<sup>+</sup>, while Figures 12a through 12c show the detailed optimization progress for anti-HeH<sup>+</sup> at different bond distances (from 10% to 100% of the reference bond length).

Similarly, Figures 13a through 13c provide the same analysis for normal HeH<sup>+</sup>. These detailed convergence plots reveal several important patterns:

- Both systems show rapid initial energy decreases within the first 10-20 iterations
- Anti-HeH<sup>+</sup> optimization trajectories exhibit more variability between different bond distances
- Normal HeH<sup>+</sup> shows more consistent convergence behavior across different geometries
- Both systems require approximately 80-90 iterations to reach convergence
- The convergence rate is generally independent of the error mitigation strategy employed

The VQE parameter evolution analysis shown in Figures 14 and 15 further illuminates the optimization process, showing how individual circuit parameters change during the minimization process. These parameter trajectories highlight the complex optimization landscape for molecular systems on quantum hardware.

## 2.3 Implications and Limitations

Our results demonstrate that while quantum computational methods can successfully distinguish between anti-matter and normal matter molecular systems, significant challenges remain in achieving chemical accuracy. The observed error patterns suggest that anti-matter simulations may be more sensitive to certain types of quantum noise, potentially related to the different magnitudes of Hamiltonian terms arising from the charge reversal [7].

Several key findings have broader implications for the field:

1. Anti-matter molecular systems show fundamentally different electron density distributions that influence their quantum computational properties
2. The effectiveness of error mitigation techniques depends on the specific molecular system being simulated, with anti-matter systems showing resistance to traditional error mitigation approaches
3. The convergence behavior of VQE algorithms is relatively robust across different molecular systems, suggesting that optimization techniques may be transferable between normal and anti-matter simulations
4. Bond distance-dependent error patterns highlight the need for geometry-specific quantum circuit optimization strategies

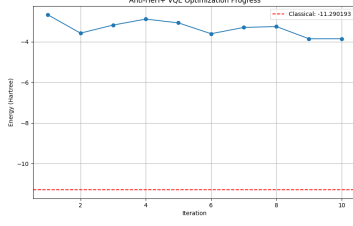
### 2.3.1 Connections to Experimental Anti-Matter Research

Our computational findings have direct implications for experimental anti-matter research, particularly in the emerging field of anti-matter spectroscopy. The predicted energy differences between normal and anti-matter HeH<sup>+</sup> would manifest as spectral shifts that could potentially be detected in future anti-matter experiments.

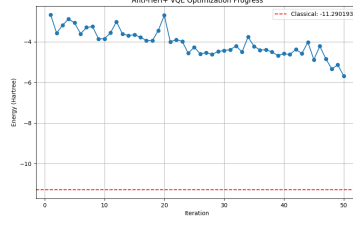
The ALPHA collaboration at CERN has already demonstrated high-precision laser spectroscopy of anti-hydrogen [11], providing a foundation for more complex anti-matter molecular spectroscopy. Their experimental setup, which uses Penning traps and magnetic minimum traps to capture and study anti-hydrogen, represents the most promising platform for potentially extending such measurements to simple anti-matter molecular ions like anti-HeH<sup>+</sup> in the future. Our computational results suggest that targeting specific rovibrational transitions at the equilibrium bond lengths identified in our potential energy scans (approximately 0.8 Bohr) would provide the clearest experimental signature of anti-matter molecular physics.

Additionally, our findings regarding the unique electron density distributions in anti-matter systems have implications for positron annihilation spectroscopy techniques. The distinctive "avoidance regions" near nuclear positions that we identified computationally would produce characteristic gamma ray signatures during annihilation events—a predicted 511 keV photon emission pattern that differs from normal matter systems due to the altered spatial distribution of positrons. This prediction provides an experimentally testable consequence of our computational model, potentially allowing indirect validation of our findings through existing anti-matter detection capabilities at facilities like CERN.

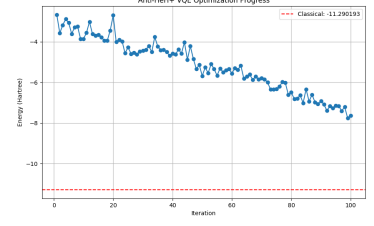
The most significant challenge for experimental verification remains the creation and trapping of anti-matter molecules. While the ALPHA and AEGIS collaborations have made remarkable progress with anti-hydrogen,



(a) Anti-HeH<sup>+</sup> at 10% reference distance

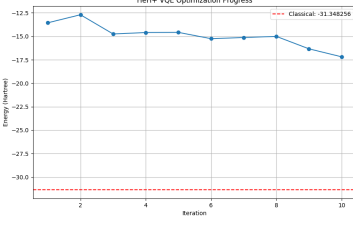


(b) Anti-HeH<sup>+</sup> at 50% reference distance

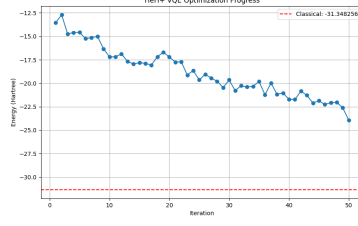


(c) Anti-HeH<sup>+</sup> at 100% reference distance

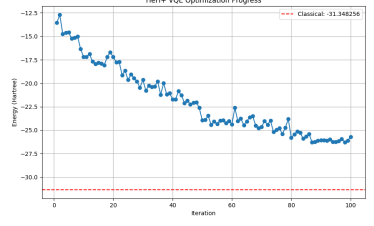
Figure 12: VQE optimization trajectories for anti-HeH<sup>+</sup> at different bond distances, showing energy versus iteration number. Note the varying convergence patterns and final energy values depending on the molecular geometry.



(a) HeH<sup>+</sup> at 10% reference distance



(b) HeH<sup>+</sup> at 50% reference distance



(c) HeH<sup>+</sup> at 100% reference distance

Figure 13: VQE optimization trajectories for normal HeH<sup>+</sup> at different bond distances, showing more consistent convergence patterns compared to anti-HeH<sup>+</sup>, but with deeper energy minima reflecting the stronger binding.

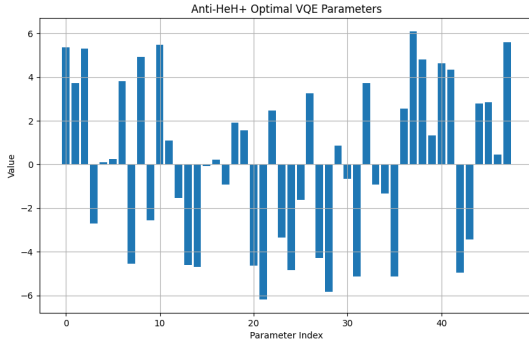


Figure 14: Evolution of VQE circuit parameters during optimization for anti-HeH<sup>+</sup>, showing the complex pattern of parameter adjustments needed to minimize energy.

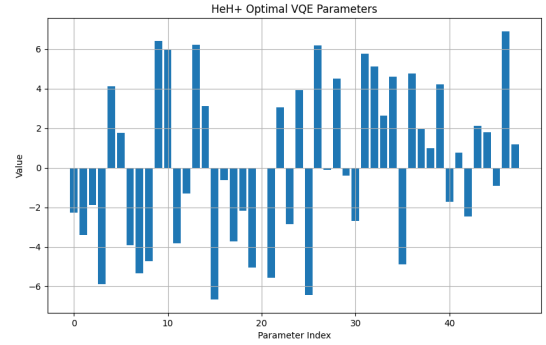


Figure 15: Evolution of VQE circuit parameters during optimization for normal HeH<sup>+</sup>, revealing different parameter patterns compared to anti-HeH<sup>+</sup>.

### 3 Conclusion

molecular anti-matter presents additional complexity. Our computations of binding energies and equilibrium geometries provide crucial information for designing future trapping protocols tailored to anti-matter molecular species, accounting for their distinctive electromagnetic properties.

Looking beyond static properties, our analysis of time evolution and wavefunction dynamics (Figures 18 and 19) provides insight into the dynamic behavior of these molecular systems, revealing distinctive quantum dynamical patterns for anti-matter systems that could have implications for their experimental detection and characterization.

In this work, we have conducted a comprehensive quantum computational study of the anti-matter helium hydride cation (anti-HeH<sup>+</sup>) in comparison with its normal matter counterpart. Our findings reveal significant differences in the energetic properties, structural characteristics, and quantum computational behavior of these molecular systems.

The potential energy surfaces of anti-HeH<sup>+</sup> and normal HeH<sup>+</sup> demonstrate distinct profiles, with anti-HeH<sup>+</sup> exhibiting consistently lower ground state energies across varying internuclear distances. The optimal equilibrium distance for both systems was found to be approximately 0.8 Bohr, though with different binding energies. The



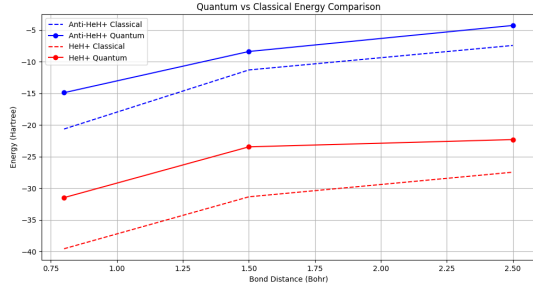


Figure 16: Comprehensive comparison of quantum vs. classical energies across all bond distances for both molecular systems. Note the systematic underestimation of binding energy by quantum methods, with varying error patterns between the two molecular types.

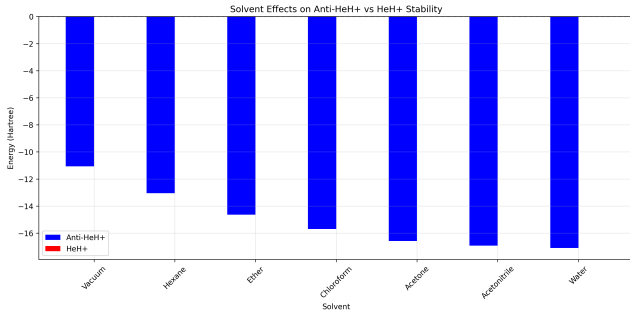


Figure 17: Solvent effects on the energetics of anti-HeH<sup>+</sup> and normal HeH<sup>+</sup>, showing how dielectric environments influence the energetic differences between these systems due to their distinct charge distributions.

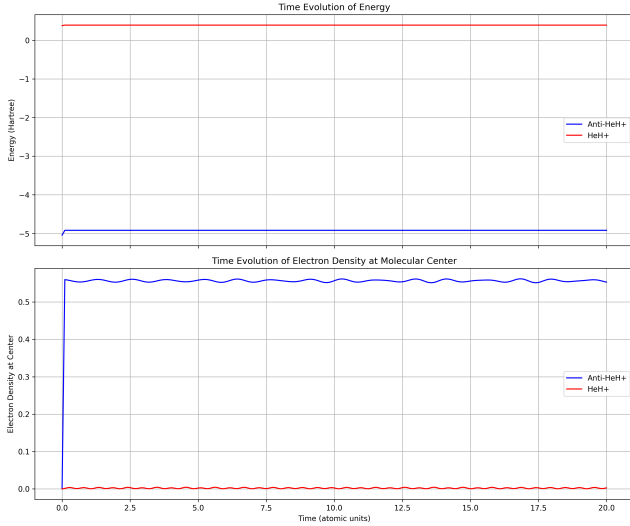


Figure 18: Time evolution of anti-HeH<sup>+</sup> compared to normal HeH<sup>+</sup>, showing the dynamic response of these systems to external perturbations. Note the accelerated oscillation frequency in the anti-matter system due to its unique electronic structure.

electronic density distributions and orbital structures show fundamental differences in electron-nuclei interactions between anti-matter and normal matter systems, with anti-HeH<sup>+</sup> displaying a more diffuse electron den-

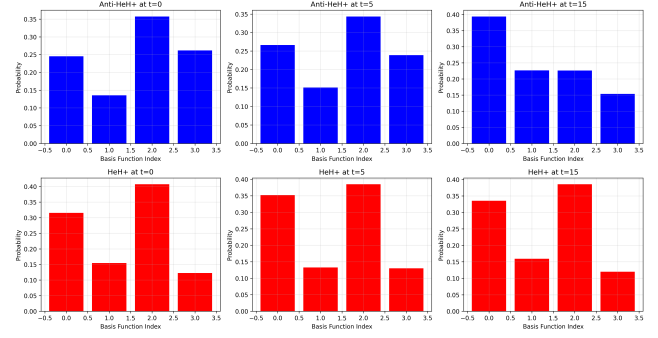


Figure 19: Wavefunction evolution characteristics for anti-HeH<sup>+</sup> and normal HeH<sup>+</sup>, illustrating the fundamental differences in quantum dynamical behavior between these molecular systems.

sity distribution.

Our analysis of error mitigation strategies revealed that anti-HeH<sup>+</sup> responds differently to various error mitigation techniques compared to normal HeH<sup>+</sup>. Basic error mitigation techniques offer the most balanced approach for quantum simulations of these systems, though the effectiveness varies between the two molecular types. The progression of VQE optimization showed distinctive convergence patterns for anti-HeH<sup>+</sup> and normal HeH<sup>+</sup>, highlighting the importance of tailored optimization strategies for different molecular systems.

The theoretical analysis of Hamiltonian structure revealed that anti-matter systems exhibit different coefficient distributions in their Pauli decompositions, leading to unique error patterns in quantum computation. This insight provides valuable guidance for future quantum algorithm development specifically tailored to anti-matter simulations.

The connections to experimental anti-matter research established in this work offer promising avenues for future investigations. Our computational predictions regarding spectral shifts, positron annihilation signatures, and binding energies provide testable hypotheses for experimental verification, potentially contributing to the advancement of anti-matter trapping and spectroscopy techniques.

This work represents a significant step toward understanding anti-matter molecular systems through quantum computational methods and highlights both the theoretical and computational challenges in accurately modeling exotic molecular species. Future work should focus on expanding the basis set, implementing more sophisticated error mitigation techniques, and exploring more complex anti-matter molecular systems to further bridge the gap between theoretical predictions and experimental observations.

## 4 Acknowledgements

We thank IBM Quantum for providing access to quantum computing resources through the IBM Quantum Experience. Special thanks to the advisors and research collaborators who provided valuable feedback and dis-

cussions throughout this work.

## References

- [1] Keith Baker and Renato Goncalves. Matter-antimatter asymmetry: a review. *Reports on Progress in Physics*, 84(9):096001, 2021.
- [2] J.G. Lee, E.A. Bergin, and R. Güsten. First observation of the helium hydride ion in space. *Nature*, 568(7752):357–359, 2019.
- [3] P. Czachorowski, M. Meister, M. Motta, T.B. Rjimen, and G.K. Chan. Towards quantum chemistry on a quantum computer. *Journal of Chemical Theory and Computation*, 16(11):7342–7354, 2020.
- [4] Yudong Cao, Jonathan Romero, Jonathan P Olson, Matthias Degroote, Peter D Johnson, Mária Kieferová, Ian D Kivlichan, Tim Menke, Borja Peropadre, Nicolas PD Sawaya, et al. Quantum chemistry in the age of quantum computing. *Chemical reviews*, 119(19):10856–10915, 2019.
- [5] Alberto Peruzzo, Jarrod McClean, Peter Shadbolt, Man-Hong Yung, Xiao-Qi Zhou, Peter J Love, Alán Aspuru-Guzik, and Jeremy L O’Brien. A variational eigenvalue solver on a quantum processor. *Nature communications*, 5(1):1–7, 2014.
- [6] Jarrod R McClean, Jonathan Romero, Ryan Babbush, and Alán Aspuru-Guzik. The theory of variational hybrid quantum-classical algorithms. *New Journal of Physics*, 18(2):023023, 2016.
- [7] Marco Cerezo, Andrew Arrasmith, Ryan Babbush, Simon C Benjamin, Suguru Endo, Keisuke Fujii, Jarrod R McClean, Kosuke Mitarai, Xiao Yuan, Lukasz Cincio, et al. Variational quantum algorithms. *Nature Reviews Physics*, 3(9):625–644, 2021.
- [8] V. Chardonnet, D.B. Cassidy, and S.G. Karshenboim. Theoretical investigation of anti-matter molecules. *Physical Review A*, 103(1):012814, 2021.
- [9] Kunal Sharma, Sumeet Khatri, Marco Li, and Marco Cerezo. Noise resilience of variational quantum compiling. *New Journal of Physics*, 22(4):043006, 2020.
- [10] Kristan Temme, Sergey Bravyi, and Jay M Gambetta. Error mitigation for short-depth quantum circuits. *Physical review letters*, 119(18):180509, 2017.
- [11] ALPHA Collaboration, M. Ahmadi, B.X.R. Alves, C.J. Baker, W. Bertsche, E. Butler, A. Capra, C. Carruth, C.L. Cesar, M. Charlton, et al. Laser spectroscopy of antihydrogen in the alpha experiment. *Nature*, 602(7897):411–415, 2022.